JOURNAL OF MATERIALS SCIENCE 26 (1991) 2389–2396

The mean intercept length polygons for systems of planar nets

G. M. LUO, A. M. SADEGH, S. C. COWIN
Department of Mechanical Engineering, The City College of The City University of New York, New York, NY 10031, USA

With a view towards the characterization of microstructural anisotropy of fibrous materials, we have shown that the mean intercept figure for a planar N-net system of straight lines is a convex $2N$-sided polygon. A very simple method of constructing the mean intercept figure for a planar N-net system is presented. It is shown, by example, that there is an inversion process by which one may construct a planar N-net system from its mean intercept polygon. The significance of these results with respect to the characterization of microstructural anisotropy of fibrous materials is discussed.

1. Introduction

The design and stress analysis of composite materials requires characterization and quantification of their microstructure. We are concerned here with composite materials containing sets of parallel fibres in different directions. In this paper we seek to quantify the directional dependence of the geometric properties of such materials. We consider the stereological method for the quantification of microstructural anisotropy called the "method of directed secants in a plane" introduced by Saltykov [1]. This method is discussed by Underwood [2]. It was applied by Whitehouse [3] to the quantification of the anisotropy on planar sections of cancellous bone specimens. Whitehouse showed that the method could be used to construct ellipses representing the microstructure of bone specimen surfaces and that the ratio of the length of the major axis to the minor axis of the constructed ellipses represented the degree of anisotropy of the spongy bone specimen, while the directions of the major and minor axes indicated the symmetry directions in the plane of the planar specimen. Harrigan and Mann [4] showed that the existence of ellipses on every face of a specimen in the form of a rectangular parallelopiped implied the existence of an ellipsoid to represent the anisotropy of the microstructure, and they noted that any ellipsoid could be represented as a second-rank tensor. Cowin [5] related a form of this second-rank tensor measure of material microstructure, called the fabric tensor, to the anisotropic elastic constants of a porous material or multiphase solid. These relationships between microstructural parameters and elastic constants were developed by Turner and Cowin [6] and shown by Cowin [7] to be consistent with similar relations based on dimensional arguments applied to structural models reported by Huber and Gibson [8]. In this paper we apply the "method of directed secants in a plane" to the quantification of the anisotropy of planar systems of straight lines. The study of planar net systems by this method was initiated by Tozeren and Skalak [9].

Although the language of this paper is pure geometry (or trigonometry), the motivation for the study is to develop a method of quantifying the directionality of a material microstructure consisting of systems of fibres in an isotropic matrix. The type and degree of mechanical anisotropy possessed by the material is directly related to directionality of the microstructure of the material. For example, if the fibres increase or decrease the stiffness and strength of the composite material, it is of interest to know the direction relative to which the axes of most fibres are closest, and the direction relative to which the axes of most fibres are most distant. The fibres in the planar net models considered here are straight lines of zero thickness.

Planar nets are sets of plane-filling parallel lines. Figs 1, 3, 5, 7 illustrate different planar net systems. A planar N-net system consists of plane-filling N sets of parallel lines. A planar single net is illustrated in Fig. 1. The single net is characterized by the angle ϕ_1 its lines make with a reference line and by the fixed distance, denoted by a_1, between each line in the set. The net direction of a single net is the direction of the line characterizing the net.

The mean intercept length of a planar net system in a specified test direction is the mean distance between intercepts of the test direction-line with the lines of the planar net system. The mean intercept length can be measured in all directions, including the net direction of each constituent planar net of the net system. A polar plot of each mean intercept length as a function of direction yields a mean intercept figure. It will be shown here that each mean intercept figure is a convex polygon for any planar net system.

In this paper we present a general method for the construction of the mean intercept polygon for a planar N-net system. The presentation is initially inductive. In the next four sections we construct the

0022–2461/91 $03.00 + .12

mean intercept polygon for planar single, two, three and four net systems, respectively. We then generalize these results to a planar N-net system and present some lemmas that make the construction and interpretation of the mean intercept polygons quite simple. We then show that it is possible to reverse the process and construct a planar N-net system from the mean intercept polygon. We close with a discussion of these results.

2. A planar single net system

Consider the planar single net system shown in Fig. 1 and characterized by an angle ϕ_1 with the reference axes and a distance a_1 between parallel lines. For this planar single net we determine the mean intercept length, $L(\theta)$, in the test direction θ, illustrated in Fig. 1, by calculating the number of intercepts per unit length in the test direction $N_L(\theta)$, then inverting

$$L(\theta) = \frac{1}{N_L(\theta)} \tag{1}$$

The test line in the θ direction is illustrated on the planar net in Fig. 1. The number of intercepts per unit length is easily seen to be $|\sin(\theta - \phi_1)|/a_1$, thus

$$L(\theta) = \frac{a_1}{|\sin(\theta - \phi_1)|} \tag{2}$$

The absolute value sign is necessary in Equation 2 because $N_L(\theta) = |\sin(\theta - \phi_1)|/a_1$ if $0 \leq (\theta - \phi_1) \leq \pi$ and $N_L(\theta) = -[\sin(\theta - \phi_1)]/a_1$ if $\pi \leq (\theta - \phi_1) \leq 2\pi$. The mean intercept length polygon is a right rectangle, two sides of which are infinite in length due to the fact that the mean intercept length becomes infinite for $\theta = \phi_1$ and $\theta = \phi_1 + \pi$ in a planar single net system. The mean intercept length polygon, which is a polar plot of $L(\theta)$ given by Equation 2, is shown in Fig. 2. A typical polar direction, θ, and $L(\theta)$ are indicated in the figure. This unboundedness of the mean intercept length polygon is not typical and only occurs for the planar single net system.

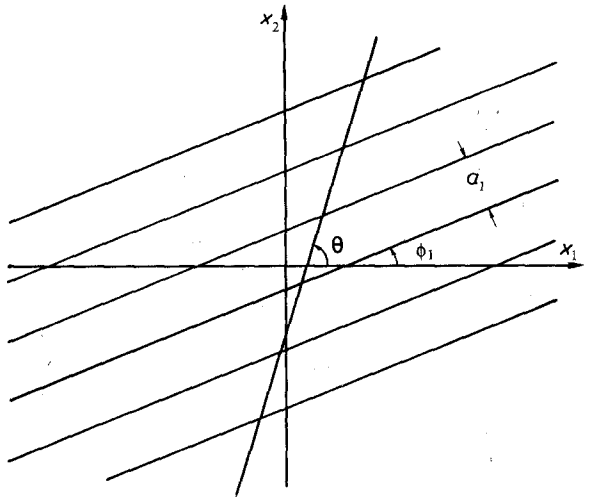

Figure 1 A planar single net system characterized by an angle ϕ_1 with the reference axes and a distance a_1 between parallel lines. The test line is inclined at the angle θ.

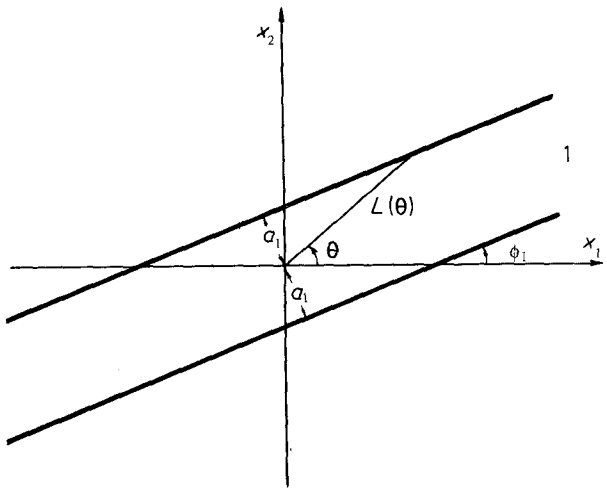

Figure 2 The mean intercept length, $L(\theta)$, figure for the planar single net system of Fig. 1.

3. A planar two net system

Consider the planar two net system shown in Fig. 3 and characterized by a net with the net direction ϕ_1 and spacing a_1 and a second net with net direction ϕ_2 and spacing a_2. The number of intercepts in the test direction θ due to intercepts with the first net is $|\sin(\theta - \phi_1)|/a_1$, and the number of intercepts in the same direction due to intercepts with the second net is $|\sin(\theta - \phi_2)|/a_2$. The sum of two numbers of intercepts in the test direction yields $N_L(\theta)$, and from Equation 1

$$L(\theta) = \frac{1}{\left[\frac{|\sin(\theta - \phi_1)|}{a_1} + \frac{|\sin(\theta - \phi_2|}{a_2}\right]} \tag{3}$$

The mean intercept length polygon is determined from a polar plot of $L(\theta)$, and the result is shown in Fig. 4. A general feature of mean intercept length polygons can be seen from this example. The vertices of the polygon lie on lines drawn from the origin that lie in the net direction of each of the constituent planar nets.

The planar single net of Fig. 1 can be recovered from the planar two net system of Fig. 3 by letting a_2 approach infinity. Increasing the value of a_2 causes points 1 and 1′ in Fig. 4 to move apart along the line 1–1′. As a_2 tends to infinity, so do the points 1 and 1′, and the lines 1′–2 and 2–1 become collinear, as do the lines 1′–2′ and 2′–1, and these two resulting straight lines are parallel. The vertices at 2 and 2′ vanish. In this way Fig. 1 for the planar single net system is recovered from Fig. 4.

As a special example of a planar two net system consider the orthogonal two net system shown in Fig. 5. In this case $\phi_1 = 0°$ and $\phi_2 = \pi/2$. The mean intercept polygon is shown in Fig. 6.

4. A planar three net system

A planar three net system is shown in Fig. 7 and its associated mean intercept length polygon is shown in Fig. 8 which is constructed for the special case when $a_1 = 1$, $a_2 = 2$, $a_3 = 3$ and $\phi_1 = 20°$, $\phi_2 = 95°$ and $\phi_3 = 135°$. The number of intercepts $N_L(\theta)$ in the

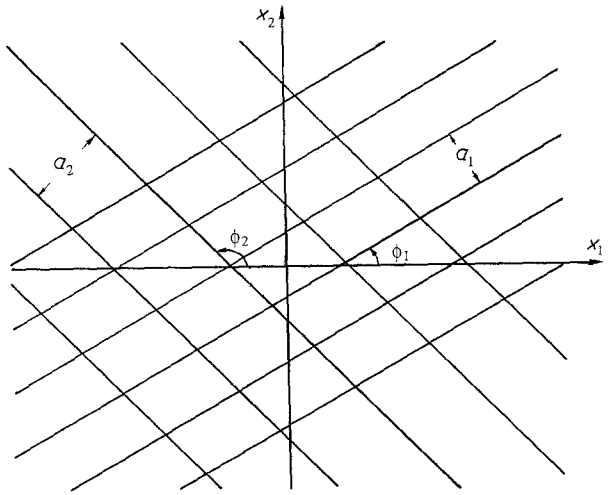

Figure 3 A planar two net system.

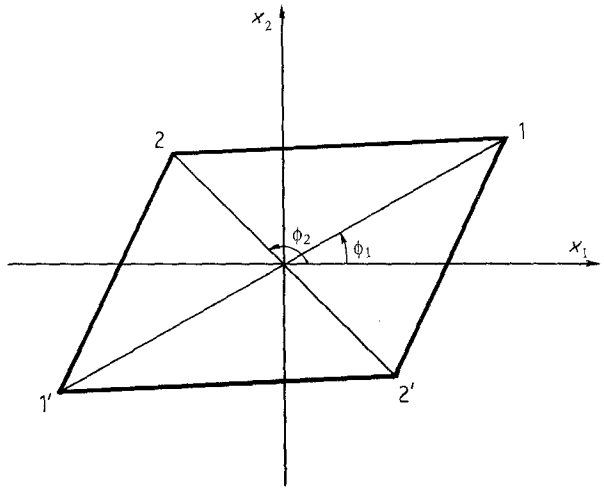

Figure 4 The mean intercept length polygon for the planar two net system.

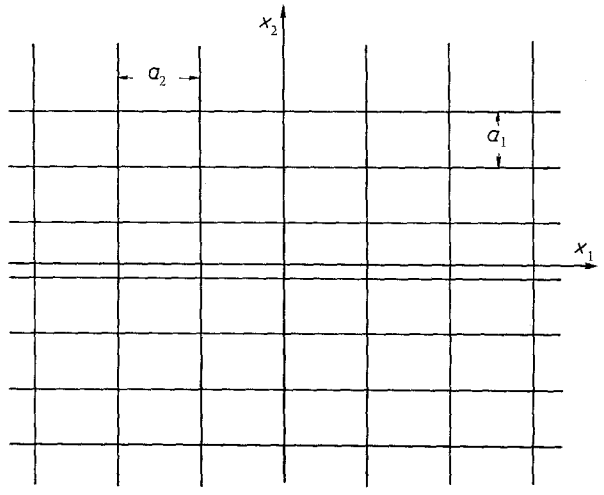

Figure 5 A planar orthogonal two net system.

test direction θ is the sum of $|\sin(\theta - \phi_1)|/a_1$, $|\sin(\theta - \phi_2)|/a_2$, and $[\sin(\theta - \phi_3)]/a_3$. Thus from Equation 1, $L(\theta)$ is given by

$$L(\theta) = 1\Big/\left[\frac{|\sin(\theta - \phi_1)|}{a_1} + \frac{|\sin(\theta - \phi_2)|}{a_2} + \frac{|\sin(\theta - \phi_3)|}{a_3}\right] \quad (4)$$

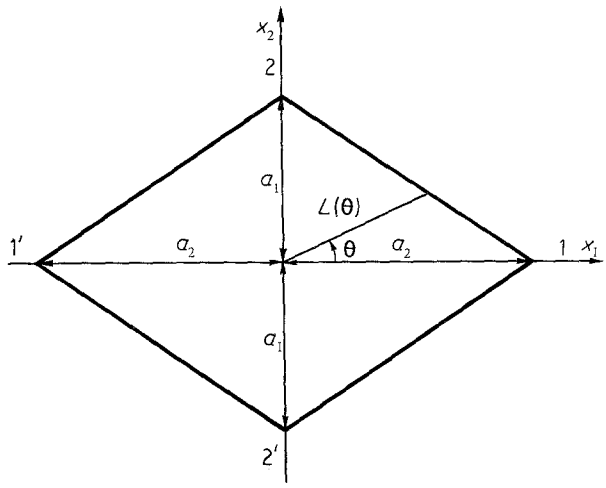

Figure 6 The mean intercept length polygon for the planar orthogonal two net system.

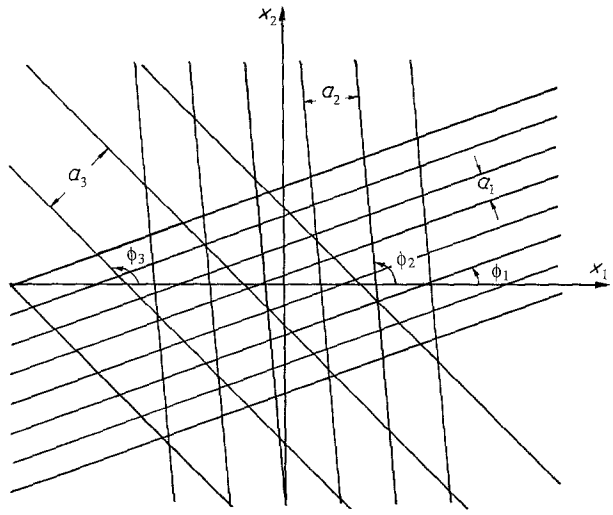

Figure 7 A planar three net system.

Along the constituent net direction lines, 1–1′, 2–2′, 3–3′ in Fig. 8, the values of $L(\theta)$ are given by

$$L(\phi_1) = 1.274 = 1\Big/\left[\frac{|\sin(\phi_1 - \phi_2)|}{a_2} + \frac{|\sin(\phi_1 - \phi_3)|}{a_3}\right] \quad (5a)$$

$$L(\phi_2) = 0.847 = 1\Big/\left[\frac{|\sin(\phi_2 - \phi_1)|}{a_1} + \frac{|\sin(\phi_2 - \phi_3)|}{a_3}\right] \quad (5b)$$

$$L(\phi_3) = 0.814 = 1\Big/\left[\frac{|\sin(\phi_3 - \phi_1)|}{a_1} + \frac{|\sin(\phi_3 - \phi_2)|}{a_2}\right] \quad (5c)$$

Observe that the mean intercept length polygon of Fig. 8 can be constructed from the data set consisting of net directions ϕ_1, ϕ_2, ϕ_3 and the mean intercept lengths $L(\phi_1)$, $L(\phi_2)$ and $L(\phi_3)$. The method of construction is to locate the six vertices of the polygon and draw straight lines connecting the vertices. The

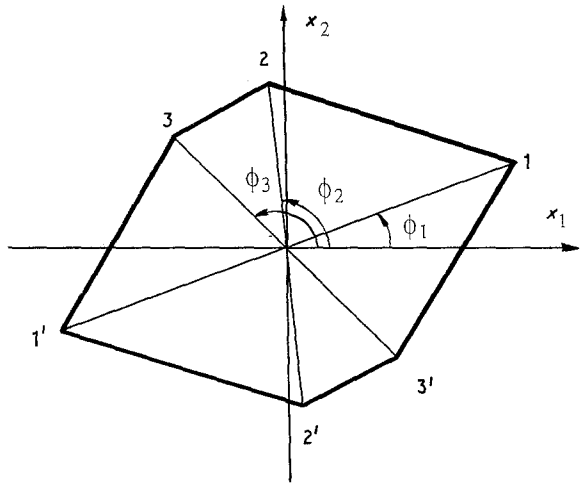

Figure 8 The mean intercept length polygon for the planar three net system.

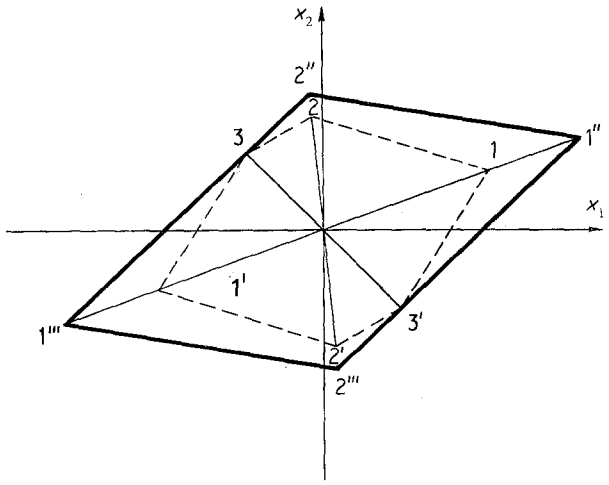

Figure 9 An illustration of the transition from the mean intercept length polygon for a planar three net system to that for a two net system obtained by allowing the spacing between the parallel lines of one net of the three net system to become very large (infinite).

vertices are located at $L(\phi_i)$ in the directions ϕ_i and $\phi_i + \pi$, $i = 1, 2, 3$.

We consider now the changes in Fig. 8 if we allow the spacing between the parallel lines in the third set, a_3, to become infinite. These changes are indicated in Fig. 9. The vertices associated with ϕ_3 vanish because the two lines 1'–3 and 3–2 of Fig. 8 become collinear, as do the two lines 2'–3' and 3'–1. The points 1 and 1' of Fig. 8 move away from the origin to 1'' and 1''', respectively, as illustrated in Fig. 9. Similarly, points 2 and 2' of Fig. 8 move outward to points 2'' and 2''' of Fig. 9. The outward movement corresponds to increases in the mean intercept length in these directions. The mean intercept length increases because the intercepts with the third net set no longer exist. The new mean intercept length polygon of Fig. 9 is one associated with a planar two net system, like the mean intercept length polygon of Fig. 4.

5. A planar four net system

A planar four net system is shown in Fig. 10. The associated mean intercept length polygons for various

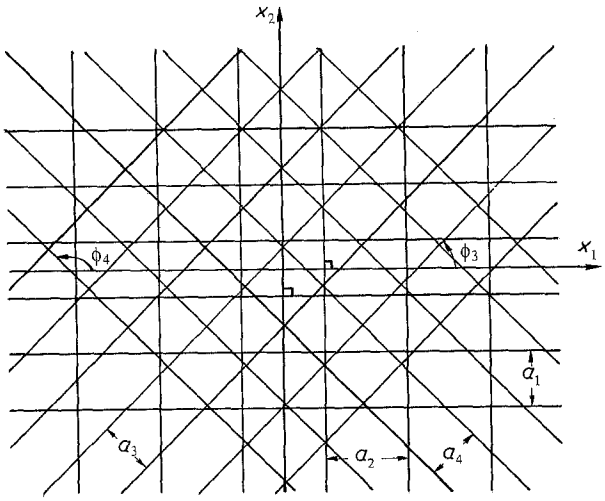

Figure 10 A planar four net system.

special values of a_1, a_2, a_3 and a_4 are shown in Fig. 11. The innermost mean intercept length polygon shown in Fig. 11 is for the special case when $a_1 = a_2 = a_3 = a_4$. The sequence of mean intercept length polygons exterior to the innermost are obtained by increasing a_2 and holding $a_1 = a_3 = a_4$ constant. The sequence of associated mean intercept length polygons grows larger anisotropically as shown in Fig. 11. The growth is characterized by the points 2 and 2' remaining fixed and the points 1 and 1' moving the greatest distance with increasing values of a_2. The associated mean intercept length polygon for the special case when $a_1 = a_2 = a_3 = a_4$ is shown in Fig. 12. When the magnitudes of $a_1 = a_2 = a_3 = a_4$ are increased uniformly the polygon grows large isotropically or uniformly as shown in Fig. 12. Note that the innermost mean intercept length polygon shown in Fig. 11 is the same as the innermost one illustrated in Fig. 12.

6. Generalization to a planar *N*-net system

For N sets of fibres in a planar net system the mean intercept length $L(\theta)$ is obtained by induction as

$$L(\theta) = 1 \Big/ \left[\sum_{i=1}^{N} \frac{|\sin(\theta - \phi_i)|}{a_i} \right] \qquad (6)$$

where a_i and ϕ_i, for $i = 1, 2, \ldots, N$, are the line spacing distance and direction of the ith single planar net, respectively. Other conclusions can be obtained by induction from the results of the previous four sections. First, for a planar N-net system ($N > 1$), the mean intercept length polygon has $2N$ sides and $2N$ vertices. As the number N of constituent nets increases, the area enclosed by the mean intercept length polygon decreases.

We shall now give a rigorous proof that the mean intercept length figure for a planar net system characterized by N distinct nets (a_i, ϕ_i), $i = 1, 2, \ldots, N$, is a polygon of $2N$ sides. First, from the definition of the mean intercept length $L(\theta)$ given by Equation 6, it follows that the $2N$ points, $L(\phi_i)$ at ϕ_i and $\phi_i + \pi$ for $i = 1, 2, \ldots, N$, lie on the boundary of the mean intercept length figure. As we have not yet shown that

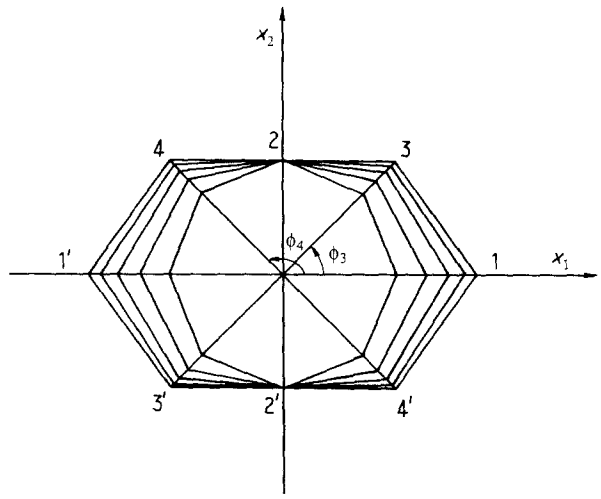

Figure 11 Mean intercept length polygons for the planar four net system of Fig. 10. The polygons in this system are generated by increasing the value of a_2. This causes the sequence of polygons to increase anisotropically.

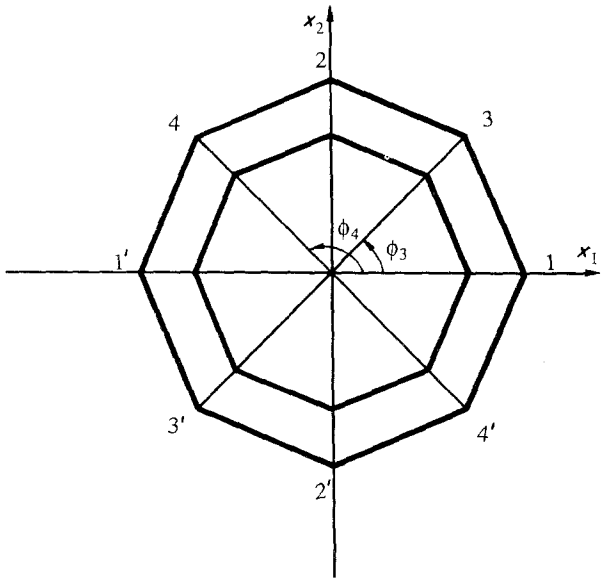

Figure 12 Mean intercept length polygons for the planar four net system of Fig. 10 in the special case when $a_1 = a_2 = a_3 = a_4$. The outer mean intercept length polygon is obtained from the inner one by increasing $a_1 = a_2 = a_3 = a_4$ uniformly, or isotropically. Note that the most central mean intercept length polygon is the same shape as the mean intercept length polygons of Fig. 11.

these points will be the vertices of the polygon, we shall refer to them as selected boundary points. Using these selected boundary points we prove the following three lemmas.

6.1. Lemma 1: the boundary of the mean intercept figure for a planar *N*-net system is a straight line between any two adjacent selected boundary points

Proof: the mean intercept length between any two selected adjacent boundary points, say K and $K + 1$, is given for $\phi_K \leq \theta \leq \phi_{K+1}$ by

$$L_K(\theta) = 1 \Big/ \left[\sum_{i=1}^{K} \frac{\sin(\theta - \phi_i)}{a_i} - \sum_{i=K+1}^{N} \frac{\sin(\theta - \phi_i)}{a_i} \right] \quad \phi_K \leq \theta \leq \phi_{K+1} \tag{7}$$

This formula is obtained from Equation 6 by evaluating the absolute value signs in the terms $|\sin(\theta - \phi_i)|$ using the now restricted range of θ, namely $\phi_K \leq \theta \leq \phi_{K+1}$. Expansion of the sine function using the trigonometric identity for the sine of the difference in two angles, the right-hand side of Equation 7 can be rewritten as

$$L_K(\theta) = \frac{1}{B_K \sin\theta - C_K \cos\theta} \tag{8}$$

where

$$B_K = D_K + \frac{\cos\phi_K}{a_K} \tag{9a}$$

and

$$C_K = E_K + \frac{\sin\phi_K}{a_K} \tag{9b}$$

$$D_K = \sum_{i=1}^{K-1} \frac{\cos\phi_i}{a_i} - \sum_{i=K+1}^{N} \frac{\cos\phi_i}{a_i} \tag{10a}$$

$$E_K = \sum_{i=1}^{K-1} \frac{\sin\phi_i}{a_i} - \sum_{i=K+1}^{N} \frac{\sin\phi_i}{a_i} \tag{10b}$$

In a subsequent calculation we will need the formulae

$$B_{K-1} = D_K - \frac{\cos\phi_K}{a_K} \tag{11a}$$

$$C_{K-1} = E_K - \frac{\sin\phi_K}{a_K} \tag{11b}$$

which can be shown easily using Equations 9 and 10. Introducing the notation

$$A_K = (B_K^2 + C_K^2)^{1/2} \tag{12a}$$

$$\cos\psi_K = \frac{B_K}{A_K} \tag{12b}$$

$$\sin\psi_K = \frac{C_K}{A_K} \tag{12c}$$

Equation 8 for $L_K(\theta)$ is rewritten in the form

$$L_K(\theta) = \frac{1}{A_K \sin(\theta - \psi_K)} \quad \phi_K \leq \theta \leq \phi_{K+1} \tag{13}$$

where A_K and ψ_K are functions of a_i and ϕ_i, $i = 1, 2, \ldots, N$. Equation 13 is the polar representation of a straight line that passes through the points $[L_K(\phi_K), \phi_K]$ and $[L_{K+1}(\phi_{K+1}), \phi_{K+1}]$ (or $[L_K(\phi_K), \phi_K + \pi]$ and $[L_{K+1}(\phi_{K+1}), \phi_{k+1} + \pi]$). That Equation 13 represents a straight line can be easily seen by converting it from polar to Cartesian coordinates. Specifically, using the formulae $x = L_K \cos\theta$ and $y = L_K \sin\theta$ for the Cartesian coordinates x and y in terms of the polar coordinates L_K and θ, elimination of $\sin\theta$ and $\cos\theta$ from Equation 13 yields the expression $yA_K \cos\psi_K - xA_K \sin\psi_K = 1$ which is

easily recognized as the equation of a straight line because A_K and ψ_K are constants. This completes the proof of the lemma.

6.2. Lemma 2: the boundary of the mean intercept length figure for a planar N-net system is continuous at the selected boundary points

Proof: the mean intercept lengths $L_{K-1}(\theta)$ and $L_K\theta$ in the intervals $\phi_{K-1} \leq \theta \leq \phi_K$ and $\phi_K \leq \theta \leq \phi_{K+1}$, respectively, are given by

$$L_{K-1}(\theta) = 1\Big/\left[\sum_{i=1}^{K-1}\frac{\sin(\theta-\phi_i)}{a_i} - \sum_{i=K}^{N}\frac{\sin(\theta-\phi_i)}{a_i}\right] \quad \phi_{K-1} \leq \theta \leq \phi_K \tag{14}$$

and Equation 7. At the selected boundary point $\theta = \phi_K$, we find that these two lengths are equal

$$L_{K-1}(\phi_K) = L_K(\phi_K) = 1\Big/\left[\sum_{i=1}^{K-1}\frac{\sin(\phi_K-\phi_i)}{a_i} - \sum_{i=K+1}^{N}\frac{\sin(\phi_K-\phi_i)}{a_i}\right] \tag{15}$$

This completes the proof of this lemma.

From these two lemmas it follows that the boundary of the mean intercept length figure is a continuous curve composed of straight line segments that change direction at the selected boundary points. It follows that the mean intercept figure for any planar net system characterized by N distinct nets (a_i, ϕ_i), $i = 1, 2, \ldots, N$, is a polygon of $2N$ sides and that the vertices of the polygon are the selected boundary points.

The final point to be proved in a rigorous manner is contained in the following lemma.

6.3. Lemma 3: the MIL polygon for a planar N-net system is always convex

Proof: we consider two vertices K and $K + 1$ of the MIL polygon illustrated in Fig. 13. We begin the proof by observing that Equations 6 and 13 are identical in the interval $\phi_K \leq \theta \leq \phi_{K+1}$, therefore

$$A_K\sin(\theta-\psi_K) = \sum_{i=1}^{N}\frac{|\sin(\theta-\phi_i)|}{a_i} \qquad \phi_K \leq \theta \leq \phi_{K+1} \tag{16}$$

If we set $\theta = \phi_K$ in Equation 16 and expand the left-hand side, then using Equations 9a,b and 12 we can show

$$\sum_{i=1}^{N}\frac{|\sin(\phi_K-\phi_i)|}{a_i} = B_K\sin\phi_K - C_K\cos\phi_K = D_K\sin\phi_K - E_K\cos\phi_K \tag{17}$$

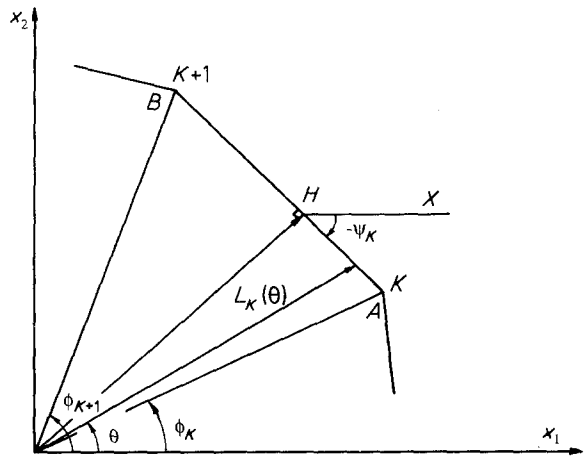

Figure 13 Two vertices, the Kth and the $(K + 1)$th, for the mean intercept length polygon of a planar N-net system.

The angle ψ_K is the angle of interest in this proof. It was introduced by Equation 13 and its negative is illustrated in Fig. 13. As we wish to prove a relationship between ψ_K and ψ_{K-1} we calculate the quantity $\sin(\psi_K - \psi_{K-1})$ by expanding the sine expression and using Equations 12a, b, c in the cases when we take K as K and when we take K as $K - 1$, thus

$$\sin(\psi_K-\psi_{K-1}) = \sin\psi_K\cos\psi_{K-1} - \sin\psi_{K-1}\cos\psi_K = \frac{1}{A_KA_{K-1}}(C_KB_{K-1} - C_{K-1}B_K) \tag{18}$$

Substitution of Equations 9a,b and 11 into Equation 18 yields

$$\sin(\psi_K-\psi_{K-1}) = \frac{2}{a_KA_KA_{K-1}}\cdot(D_K\sin\phi_K - E_K\cos\phi_K) \tag{19}$$

Finally, substitution of Equations 17 into Equation 19 yields

$$\sin(\psi_K-\psi_{K-1}) = \frac{2}{a_KA_KA_{K-1}}\cdot\sum_{i=1}^{N}\frac{|\sin(\phi_K-\phi_i)|}{a_i} \tag{20}$$

Because the quantity of the right hand side of Equation 20 is positive we have shown that

$$\sin(\psi_K-\psi_{K-1}) > 0 \tag{21}$$

This shows that $\psi_K > \psi_{K-1}$ if $0 < \psi_K - \psi_{K-1} < \pi$, which demonstrates the convexity of the polygon. This completes the proof of the lemma.

7. The inverse problem

The inverse problem is now considered, namely the construction of a planar net system from the mean intercept length figure rather than vice versa. The solution to this inverse problem is illustrated by an example. The example selected is to construct planar twelve net systems that will yield a mean intercept length polygon of 24 sides that is approximately in the

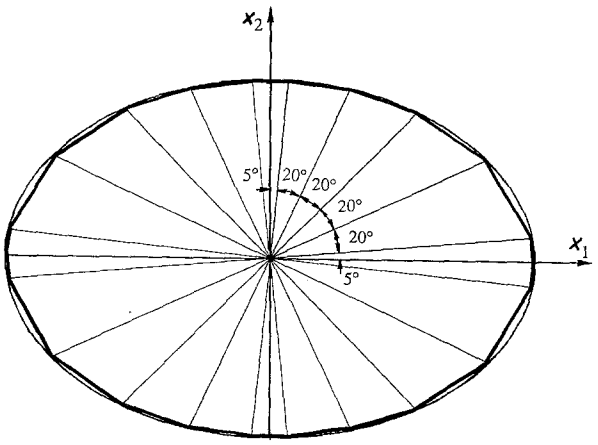

Figure 14 The mean intercept length polygon for the planar system that is chosen to approximate an ellipse.

shape of an ellipse with a major axis a and a minor axis b. The ellipse and its approximation by a 24 sided polygon are illustrated in Fig. 14.

The equation for the ellipse is $(x/a)^2 + (y/b)^2 = 1$ in Cartesian coordinates or

$$r = 1\Big/\left(\frac{\cos^2\theta}{a^2} + \frac{\sin^2\theta}{b^2}\right)^{1/2} \tag{22}$$

in polar coordinates. The major and minor axes of this ellipse are taken as $a = 1.5$ and $b = 1$, respectively. The net directions, illustrated in Fig. 14, for the 12 selected nets are $\phi_1 = 0°$, $\phi_2 = 5°$, $\phi_3 = 25°$, $\phi_4 = 45°$, $\phi_5 = 65°$, $\phi_6 = 85°$, $\phi_7 = 90°$, $\phi_8 = 95°$, $\phi_9 = 115°$, $\phi_{10} = 135°$, $\phi_{11} = 155°$ and $\phi_{12} = 175°$. The mean intercept length $L(\phi_i)$, $i = 1, \ldots, 12$, associated with each of these net directions is determined by requiring that the value of $L(\phi_1)$ lie on the curve of the specified ellipse. The formula for this follows from Equations 6 and 22, thus

$$L(\phi_j) = 1\Big/\sum_{i=1}^{12}\frac{|\sin(\phi_j - \phi_i)|}{a_i}$$

$$= 1\Big/\left(\frac{\cos^2\phi_j}{a^2} + \frac{\sin^2\phi_j}{b^2}\right)^{1/2} \qquad j = 1, \ldots, 12 \tag{23}$$

In the system of 12 Equations 23, there are 12 unknowns, the 12 a_i. All the other quantities, a and b and the ϕ_i, $i = 1, \ldots, 12$, have been specified. Actually, because of the symmetry in the problem (i.e. $L(0°) = L(180°)$, $L(5°) = L(175°)$, $L(25°) = L(155°)$, $L(45°) = L(135°)$, $L(65°) = L(115°)$ and $L(85°) = L(95°)$) there are only seven distinct a_is to find. These a_is are given by $a_1 = 15.31$ for $L(0°) = L(180°)$, $a_2 = 6.483$ for $L(5°) = L(175°)$, $a_3 = 5.108$ for $L(25°) = L(155°)$, $a_4 = 7.663$ for $L(45°) = L(135°)$, $a_5 = 10.69$ for $L(65°) = L(115°)$, $a_6 = 19.78$ for $L(85°) = L(95°)$ and $a_7 = 51.48$ for $L(90°)$. The resulting planar twelve net system is illustrated in Fig. 15.

8. Discussion

Results concerning the mean intercept figures for planar N-net systems have been developed for the purpose of characterizing the microstructural anisotropy of fibrous materials. With some degree of rigour we have shown that the mean intercept figure for a planar N-net system is a convex $2N$-sided polygon. We have illustrated a very simple method of constructing the mean intercept figure for a planar N-net system. Further we have shown, by example, that there is an inversion process by which one may construct a planar N-net system from its mean intercept polygon.

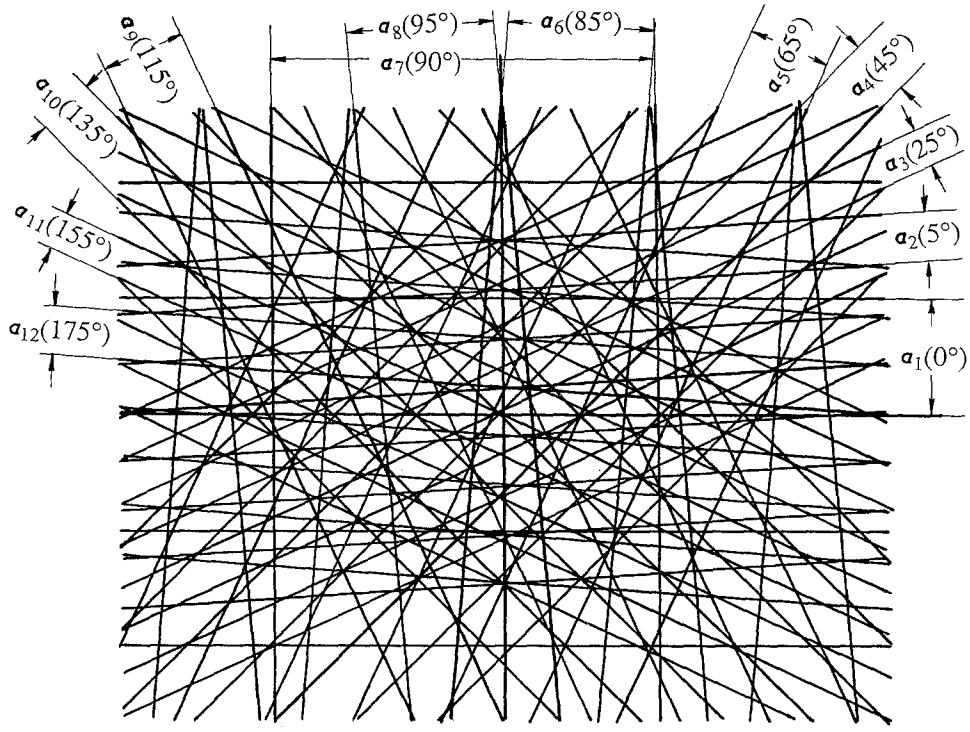

Figure 15 The planar twelve net system whose mean intercept length polygon approximates the ellipse of Fig. 14.

An alternate approach to the characterization of microstructural anisotropy is to construct a polar plot of the number of intercepts per unit length, $N_L(\theta)$, in the test direction θ rather than a polar plot of the mean intercept length $L(\theta)$ in the test direction θ. The polar plot of the number of intercepts per unit length $N_L(\theta)$ produces a figure called the "rose-of-the-number-of-intersections". Underwood [10] investigates the characterization of the anisotropy of planar net systems using the rose-of-the-number-of-intersections. A comparison of the two methods can be obtained easily by comparing the mean intercept length polygons given here with the rose-of-the-number-of-intersections plots given by Underwood for the same planar net systems. One advantage of the mean intercept length approach is the representation of the result by a convex polygon so that it is easy to evaluate visually the more pronounced and less pronounced directions of fibre orientation. A second advantage of the mean intercept length approach is the inversion algorithm described here. From this result it is easy to see how it is possible to increase the number of nets in the planar net system to infinity and still have a prescribed type of anisotropy in the mean intercept length figure. Intuition suggests that as the number of planar net systems becomes arbitrarily large, the mean intercept length figure should become circular, suggesting isotropy. Underwood [10] makes a remark to this effect on p. 108. However, using the inversion algorithm it is easy to see that one can construct a planar net system with an arbitrarily large number of nets that has any closed convex curve as its mean intercept length figure. We presented the case of an ellipse and a twelve net system here, and it easy to see how this method extends to any closed convex curve and any number of planar net systems.

Acknowledgement

This investigation was supported by NSF Grant no. BSC-8822401. This research was also supported (in part) by grant no. 669301 from the PSC-CUNY Research Award Program of the City University of New York. We thank Mr Yves Arramon for comments on an earlier draft of this manuscript.

References

1. S. A. SALTYKOV, "Stereometric Metallography" (State Publishing House for Metals and Sciences, Moscow, 1958).
2. E. E. UNDERWOOD, "Quantitative Stereology" (Addison Wesley, Reading, MA, 1970).
3. W. J. WHITEHOUSE, *J. Microscopy* **101** (1974) 153.
4. T. P. HARRIGAN and R. W. MANN, *J. Mater. Sci.* **19** (1984) 761.
5. S. C. COWIN, *Mech. Mater.* **4** (1985) 137.
6. C. H. TURNER and S. C. COWIN, *J. Mater, Sci.* **22** (1987) 3178.
7. S. C. COWIN, *ibid.* in press.
8. A. T. HUBER and L. J. GIBSON, *ibid.* **23** (1988) 3031.
9. A. TOZEREN and R. SKALAK, *ibid.* **24** (1989) 1700.
10. E. E. UNDERWOOD, "Quantitative Microscopy", edited by R. T. De Hoff and F. N. Rhines (McGraw Hill, New York, 1968).

Received 27 June
and accepted 1 August 1990